HYBRID EXPERIMENTS ON EARTHQUAKE FAILURE CRITERIA OF REINFORCED CONCRETE STRUCTURES

Hirokazu IEMURA

SUMMARY

In this study, on-line hybrid experiments are conducted in which earthquake response is calculated by a digital computer adopting the real hysteretic restoring force of a reinforced concrete bending structural element directly measured from a loading actuator. Tested results show that the total absorbed energy by hysteresis loops is one of the best parameters to represent deterioration process of stiffness, strength and energy absorbing capacity of structural elements. Correlation of conventional and new damage and failure criteria are examined for theoretical and practical earthquake damage assessment of structures. Tested specimens are repaired by grouting of the epoxy resin and reloaded with the same eathquake motion as the original one to find restoration of the resistance. It is verified from the results that even a specimen of which concrete is severly crushed can well be repaired.

1. INTRODUCTION

In earthquake resistant design of most structures, it is a common approach to produce a structure capable of responding to moderate shaking (more than a few times expected intensity of excitation in its life time) without damage, and capable of resisting the unlikely event of very strong shaking without seriously endangering the occupants. In the second case, it is necessary to investigate earthquake response properties of structures beyond yielding, limit approaching to failure.

When hysteresis loops of restoring forces of structures do not deteriorate during earthquake response, a large amount of energy absorption is expected to suppress their dynamic response, so that aseismic design of structures becomes possible with relatively low yielding level, as has been suggested by Newmark et al. (1). This may be the case for ductile structures like steel framed buildings.

For reinforced concrete or composite structures, however, increasing emphasis has been given to deterioration effects during earthquake response on the basis of recorded seismograms (2) and loading tests of structural elements (3). For those structures, two fundamental researches are needed : (a) how to represent deterioration process of structural resistance, and (b) what are appropriate damage and failure criteria. The author has been involved in analytical and experimental studies in this field (4,5) and this paper presents the latest results with a newly developed on-line hybid testing system.

2. HYBRID SYSTEM FOR ON-LINE EARTHQUAKE RESPONSE ANALYSIS

The equation of motion of hysteretic structures is written in the next form as,

$$\underline{M}\ddot{\underline{X}}(t) + \underline{C}\dot{\underline{X}}(t) + \underline{F}(\underline{X}(t)) = -\underline{M}\{1\}\ddot{Z}_B(t) \quad \ldots\ldots\ldots\ldots\ldots(1)$$

Associate Professor, Department of Civil Engineering, Kyoto University, Kyoto, 606, JAPAN

where, $\underline{M}$: mass matrix
$\underline{X}(t)^t=(x_1,.....,x_n)$: relative displacement vector at time t
$\underline{C}$: damping matrix
$\underline{F}(\underline{X}(t))$: hysteretic restoring force vector
$\ddot{z}_B$: ground acceleration

In solving Eq. (1), $\underline{F}(\underline{X}(t))$ has been mathematically modeled using results of static and dynamic loading tests. Although a lot of efforts and sophisticated techniques are needed in modelling $\underline{F}(\underline{X}(t))$, some errors can not be avoided. If we can adopt $\underline{F}(\underline{X}(t))$ directly from a loading actuator and calculate Eq.(1), this technique is one of the most accurate estimations of earthquake response. This is the basic idea of hybrid on-line earthquake response analysis (6,7).

The on-line hybrid system is schematically illustrated in Fig.1, where analog and digital data are exchanged through DA and AD convertor. The specimens were simply supported by a pair of cylinders and constant axial force was generated by the system shown in Fig.2 and Photo 1, in which oil pressure was kept constant with air pressure regulator. The relation between displacement δ and restoring force f at the center of the specimen shown in Fig.3(a) is adopted as $f(x_i)$ in Eq.(1). This relation between f and δ is supposed to represent that of the bridge pier shown in Fig.3(b).

3. SPECIMENS AND INPUT EARTHQUAKE ACCELERATION

In the experiment, reinforced concrete specimens shown in Fig.4 which have cross section of 150x100mm and span-length of 1500mm were used. Four longitudinal reinforcing bars (9.5mm and 16.0mm) are placed, equivalent to a reinforcement ratio p of 1.1 % and 3.1 %, respectively. Lateral tie hoops (6.0mm) are placed every 70mm to prevent shear failure. The axial force was controlled so as to generate conpressive stress σ_c of concrete ranging from 10 to 20 kg/cm^2.

As input earthquake excitation, two earthquake accelerograms were used. One is the NS component of El Contro record during Imperial Valley earthquake (5-18-1940) in the U.S. and the other is NS component of Hachinohe record during Tokachioki earthquake (5-16-1968) in Japan. Maximum acceleration of the two accelerograms are set in the range from 100 to 300 gal (=cm/sec^2).

Types of specimens and cases of the experiments are summarized in Table 1. In total, 30 hybrid experiments of earthquake response were conducted. Results of static load-displacement relation of all types of the specimens are shown in Table 1, from which it is found that ductility of the specimens becomes lower with the higher reinforcement ratio and with the larger axial stress. It was also noted that cracking and yielding loads of the specimens become higher with the larger axial stress due to the same principle as prestressed RC beams. These load-displacement relation agreed well with analytical results.

4. EARTHQUAKE HYSTERETIC RESPONSE OF RESTORING FORCE AND DETERIORATION PROCESS OF STRUCTURAL RESISTANCE

In Fig.5, the calculated hysteretic response of restoring force subjected to the El Centro accelerogram record with maximum value of 200 gal in duration of 30 seconds is plotted for SC-1, 2 and 3. The natural period and damping ratio of the structural model in the elastic range were set at 0.5 seconds and 5 %, respectively. The intensity parameter γ shows the ratio of maximum input acceleration to yielding acceleration of the specimens. The restoring force of SC-3 with no axial stress and SC-2 with low axial stress show football

shaped stable hysteresis loops. No large deterioration of the stiffness is found for SC-3 and SC-2. In these specimens, maximum ductility factor response is less than the crushing displacement but larger than the allowable displacement defined in reference 10.

The maximum ductility factor response of SC-1 with high axial stress is larger than the crushing displacement, and the hysteresis loops change from football type to inverted S type. The stiffness of the loops in small amplitude is found to be small and a pinching effect is also found.

From these three figures, it is also verified that a higher axial force results in the higher yielding level and the lower ductility of the specimens.

In Fig. 6, the relation between the stiffness deterioration ratio DS and the accumulated absorbed energy E at the end of excitation is plotted, from which the correlation is found very high. Comparing with similar plot between the maximum ductility factor response μ and E, it is verified that the accumulated energy, which is an integrated parameter during earthquake response, is a better measure for the stiffness deterioration than the maximum ductility factor response, which is a point parameter at instantaneous time.

Deterioration process of energy absorbing capacity of every half cycle is detected from a index DW_H.

$$DW_H = \sqrt{E_i/X_i^2} \,/\sqrt{E_o/X_o^2} \quad \cdots\cdots\cdots\cdots\cdots\cdots\cdots\cdots\cdots\cdots(2)$$

where, E_i: absorbed energy in every i th half cycle

X_i: amplitude of the i th half cycle

It is interesting to find the relation between DW_H and the accumulated absorbed energy from the first yielding (E_o, X_o), to the end of excitation. This relation is plotted in Fig.7 where high correlation between DH_H and E is found. This result suggests that deterioration of energy absorbing capacity can be well predicted from the total absorbed energy by hysteresis loops.

5. RESTORATION OF STRUCTURAL RESISTANCE OF REPAIRED SPECIMENS

Damaged specimens due to previous on-line hybrid loading tests were repaired by grouting of epoxy resin using the BICS (Balloon Injector for Concrete Structures) technique. The repaired specimens were subjected to exactly the same intensity and the same earthquake excitation as the original tests, in order to compare the restored structual resistance to that of the original specimens. Deterioration process of hysteresis loops were also investigated in terms of secant stiffness and accumulated hysteretic energy and damage functions as before.

When maximum acceleration of excitations were 200 gal or less, damage of original specimens were limited to cracking of concrete and tensile yielding of reinforcing bars (Fig.8(a) and (b)). In this range of damage, repaired specimens are found to have almost the same structural resistance and deterioration process of hysteresis loops, although new damage was observed not at the repaired point but just next to it (Fig.9(a) and (b)). A little increase of restoring force was also detected.

For maximum acceleration of excitations 250 gal or larger, severe crushing of concrete was observed in wider range of original specimens (Fig.8(c) and (d)). In these cases, significant change of structural resistance had been expected because of the large amount of replacement of the concrete material. However, repaired specimens have shown almost the same structural resistance and earthquake response as the original ones.

In Fig.10, hysteretic response of repaired specimens which were subjected to El Centro record with maximum acceleration of 200 gal is shown only from 0 to 5 seconds. No significant difference is noticed except an increase of restoring force, which can be explained as follows. The original damage occurred at the point where bending moment is maximum (Fig.15(a)). However second damage was detected beside the repaired region, which has high yielding strength because of epoxy resin grouting (Fig.15(b)). This means that the second damage is caused not by the maximum, but rather a smaller bending moment in the specimens. Therefore, larger force is needed to let the specimens go beyond the yield point.

In Table-1, damage parameters of earthquake response of repaired specimens are shown to have almost similar values to those of original specimens. Hence, from this table it is concluded that repair work has restored asismic resistance of specimens fairly well, even for severe damage.

6. ENERGY PARTITIONING AND EARTHQUAKE FAILURE CRITERIA

Maximum value of ductility factor response has been widely used both in research and design practice for a measure of structural damage and failure, when inelastic earthquake response analyses were conducted, mainly because of its simplicity (1). As discussed in the previous sections, however, there are other parameters which can measure structural deterioration better than the conventional ductility factor response. It is the intent of this section to find a better parameter for damage and failure criteria of deteriorating hysteretic structures.

To investigate the ratio of energy absorption by hysteresis loops to total input earthquake energy, energy partitioning is calculated from next equation.

$$M\int_0^t \ddot{X}\ddot{X}dt + C\int_0^t \dot{X}^2 dt + \int_0^t F(X)dX = -M\int_0^t \ddot{Z}\ddot{X}dt \quad \text{.....(3)}$$

The first term of the left hand side of the equation is kinetic energy W_k of a structure at time t, the second is the energy absorbed by viscous damping W_D and the third is summation of the energy absorbed by hysteresis loops and the potential energy at time t, which will be denoted as W_H. The right hand side of Eq.(3) is the total earthquake input energy E to a structure.

In Fig.12, an example of partitioning of input energy is plotted using the data of the experiment. Because of yielding, W_H is found much larger than W_C. The top curve represents the total input energy E.

The values of E, W_H and W_H/E at the end of earthquake excitation with different intensity are plotted in Fig.13. It is natural to find that E and W_H increase with intensity of the excitation. However, W_H/E shows its peak around 250 gal, which suggests that the ratio of energy absorption by hysteresis loops to the total input energy has an upper limit. These peak points may be defined as the failure points from the point of view of energy participation. This definition of failure agrees better with damage of specimens inspected after the experiments than the conventional ductility factor response.

In Table 2, the maximum ductility factor response, the stiffness deterioration at the end of excitation and the hysteretic absorbed energy are shown for increasing intensity of El Centro-NS record. Analytical calculation was made by the "SAKE" program and the results are shown in parenthesis. Values with * are experimental data of repaired specimens which were explained in the previous section. Similar results are calculated and compared for

Hachinohe-NS record.

7. CONCLUSION

1) Developed on-line hybrid system is a very powerful tool to calculate earthquake response of a structure with complex and deteriorating hysteretic restoring force. Although a simple flexure beam with axial force is investigated in this study, the system can easily be extended to more complex structures with possible combinations of actuators and computers.
2) Accumulated hysteretic energy absorption is found to be the best parameter to measure deterioration process of equivalent stiffness and normalized energy absorbing capacity of structures. However, from regression analyses, conventional maximum ductility factor response is also confirmed to be a good parameter for damage assessment of deteriorating hysteretic structures.
3) Although Takeda's hysteresis model underestimates total hysteretic energy absorption compared to the experiments, maximum ductility factor response and stiffness deterioration are well predicted by the model. These results suggest that Takeda's model is useful for practical purposes.
4) Repaired specimens by grouting epoxy resin have restored almost similar resistance compared to original ones. Results verify that even a specimen for which concrete is severely crushed can be repaired, unless reinforcing bars and tie hoops are heavily damaged.

ACKNOWLEDGEMENTS

The author thanks Professor Yamada of the department of Civil Engineering of Kyoto University for his advice and encouragement in conducting this research. The author's gratitude is extended to Professor Kobayashi amd Mr. Miyagawa for their help in making and repairing test specimens, and also to graduate students, Mr. Nishimura and Mr. Suzuka for their cooperation in numerical calculation and in the experiments.

REFERENCES

1) Newmark, N.M., and Hall, W.J., "Procedures and Criteria for Earthquake Resistant Design, "Building Practices for Disaster Mitigation, National Bureau of Standars, Building Science Series No.46, pp.209-236, 1973.
2) Iemura, H. and Jennings, P.C., "Hysteretic Response of a Nine Story Reinforced Concrete Buildings," Earthquake Engineering and Structural Dynamics, Vo.13, pp.183-201, 1974.
3) Shiga, T., et al, "Experimental Study on Dynamic Properties of Reinforced Concrete Shear Walls," Proc. of 5th WCEE, Vol.I, pp.1157-1166, 1974.
4) Iemura, H., "Earthquake Failure Criteria of Deteriorating Hysteretic Structures," Proc. of 7th WCEE, Vol.5, pp.81-88, 1980.
5) Iemura, H., Kato,T. and Kawatani, Y., "Hybrid Experiments on Earthquake Response of Original and Repaired RC Memberes," Proc. of 6th Japan Earthquake Engineering Symposium, pp.825-832, Dec. 1982.
6) Hakuno, M. and Shidawara, M., "Dynamic Failure Tests of a Member by an Earthquake Type External Force," Proc. of the 3rd Japan Earthquake Engineering Symposium, pp.675-682, 1970.
7) Okada, T., Seki, M. and Yung J. Park, "A Simulation of Earthquake Response of Reinforced Concrete Building Frames to Bidirectional Ground Motion by IIS Computer Actuator Online System," Proc. of 7th WCEE, Vol.5, pp.41-48, 1980.
8) Takeda, T., Sozen, M.A., and Nielsen, N.N., "Reinforced Concrete Response to Simulated Earthquakes," Journal of the Structural Division, ASCE, Vol.96, ST12, pp.2557-2573, 1970.
9) Otani, S., "SAKE, a Computer Program for Inelastic Response of R/C Frames to Earthquakes," Civil Engineering Studies, Structural Research Series No.413, University of Illinois at Urbana Champaign, 1974.
10) Japan Road Association, "Specifications for Eathquake Resistant Design of Highway Bridges," 1980 (in Japanese).

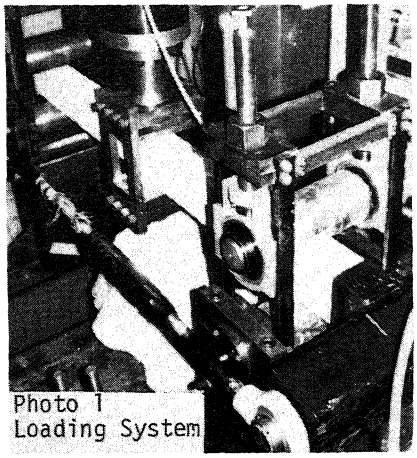

Photo 1
Loading System

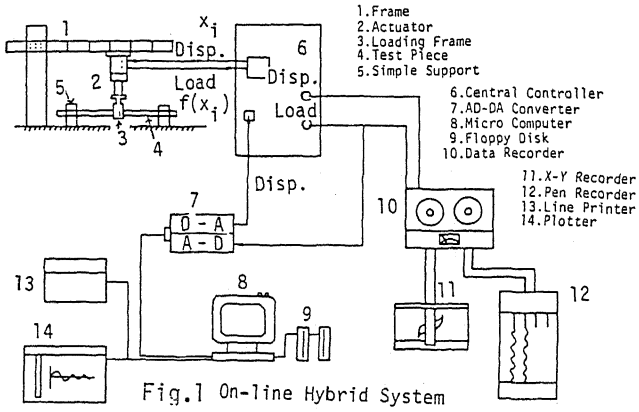

Fig.1 On-line Hybrid System

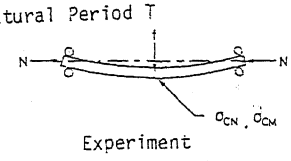

Experiment

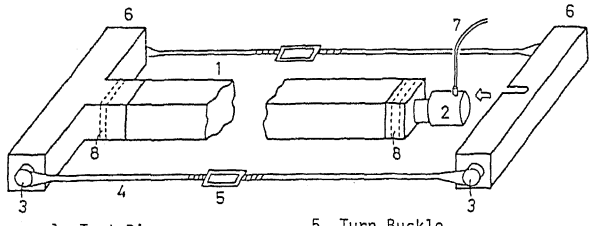

1. Test Piece
2. Oil Cylinder
3. Rotation Free Bearing
4. Tie Rod
5. Turn Buckle
6. Loading Box
7. Oil Pressure Hose
8. Rubber Cushion

Fig.2 Loading System of Axial Force

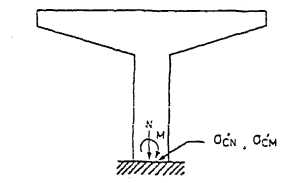

Analized Bridge Pier

Similarity

$$\begin{cases} T = T' \\ \sigma_{CN} = \sigma'_{CN} \\ \sigma_{CN}/\sigma_{CM} = \sigma'_{CN}/\sigma'_{CM} \end{cases}$$

Fig.3 Bridge Pier and its Modeling

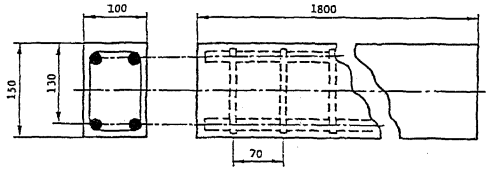

Fig.4 Test Specimen

Table 1 Types of Specimens for Tests

Types of Specimens	New or Repaired	P(%)	σ_c (Kg/cm²)	μ_D	μ_a	Earthquake Records (gal)	
						Hachinohe NS	El Centro NS
SC-1	New	1.1	20	3.65	1.22	100,150,200, 250,300	150, 200, 250, 300
SC-2	New	1.1	10	5.00	1.67		
SC-3	New	1.1	0	7.26	2.42	100,150,200, 250,300	
SC-4	New	3.1	10	3.32	1.11		
SC-5	Repaired	1.1	0	7.26	2.42		

μ_D:Ultimate Ductility Factor, μ_a:Allowable Ductility Factor in [10]

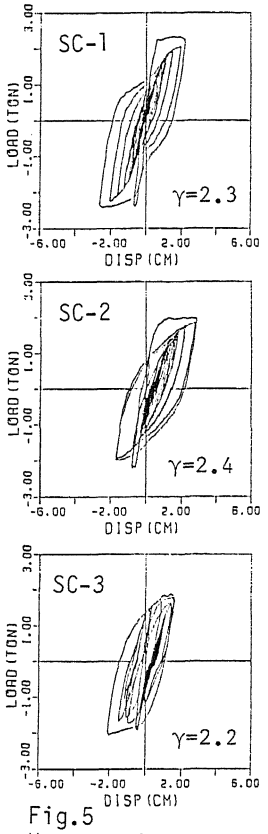

Fig.5 Hysteresis Loops with and without Axial Force

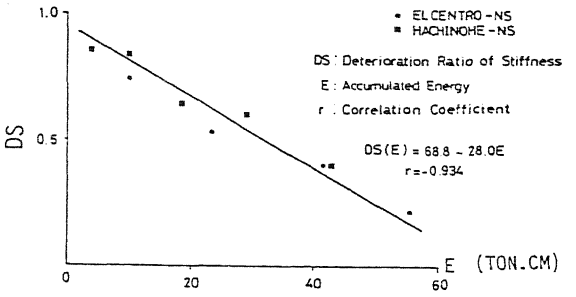

Fig.6 Accumulated Energy and Stiffness Deterioration

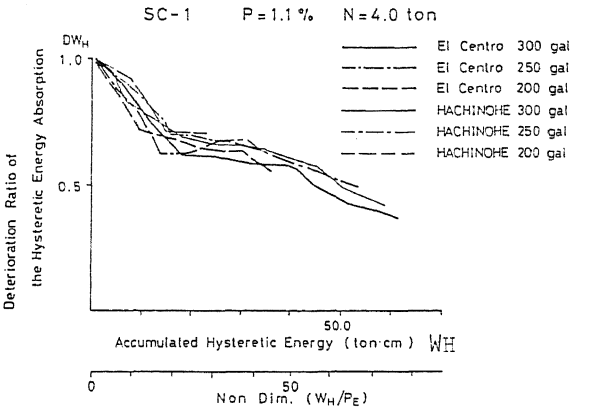

Fig.7 Deterioration of Energy Absorption

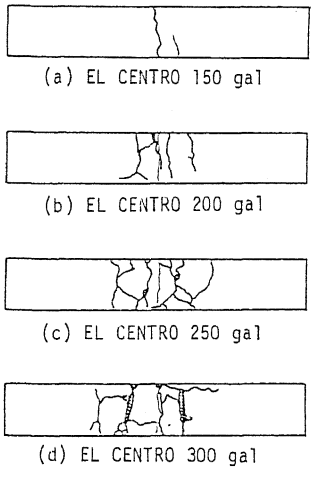

Fig.8 Original Specimens

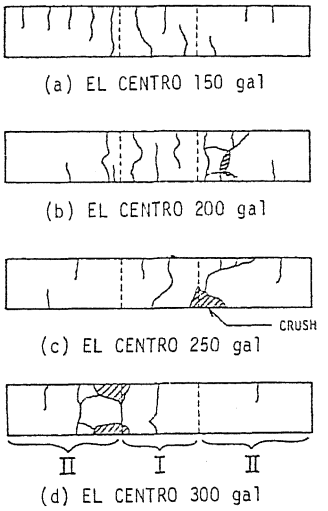

Fig.9 Repaired Specimens

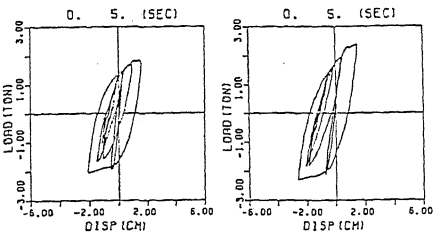

Fig.10 Hysteresis Loops

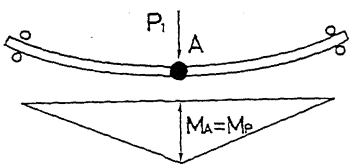

(a) Original Test Piece

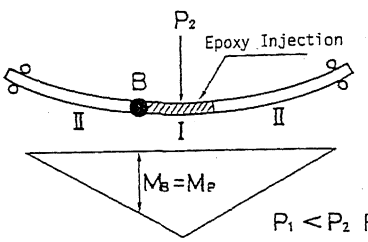

A,B : Plastic Hinge
M_p : Plastic Moment

(b) Repaired Test Piece

Fig.11
Location of Plastic Hinge

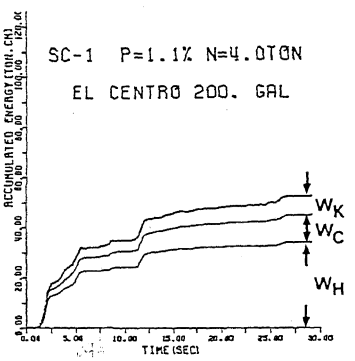

$P_1 < P_2$ Fig.12 Partitioning of Input Energy

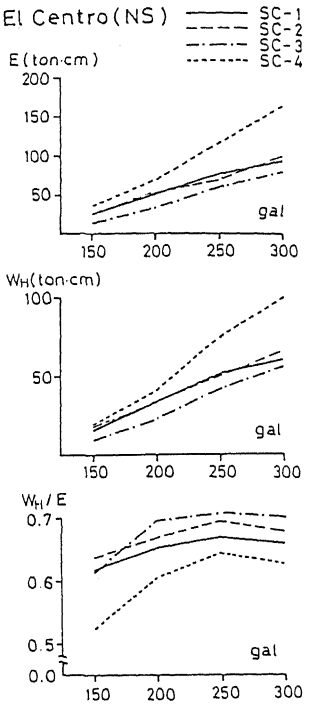

Fig.13 Input Energy and Hysteretic Absorbed Energy

Table 2 Earthquake Failure Criteria

Failure Criteria	gal / Specimens	150	200	250	300
Ductility Factor Response	SC-1	2.71	3.81	5.32	7.70
	SC-2	3.02	4.40	6.44	9.08
	SC-3	1.87 2.71* (2.31)	3.38 3.39* (3.34)	4.69 5.43* (5.48)	7.74 6.20* (6.61)
Stiffness Deterioration	SC-1	0.64	0.55	0.41	0.20
	SC-2	0.57	0.42	0.37	0.51
	SC-3	0.73 0.63* (0.65)	0.53 0.54* (0.48)	0.41 0.38* (0.40)	0.41 0.22* (0.36)
Hysteretic Absorbed Energy (ton·cm)	SC-1	16.2	34.2	51.9	61.0
	SC-2	17.8	33.9	50.6	65.5
	SC-3	9.78 11.3* (8.80)	23.2 24.5* (18.1)	41.6 47.2* (29.8)	55.6 63.2* (43.9)

*Repaired Specimens, ( )Calculated by SAKE Program